This is the Pre-Published Version.

The following publication Chen, X., Wu, S., Liu, Y., Wu, W., & Wang, S. (2022). A patrol routing problem for maritime Crime-Fighting. Transportation research part E: logistics and transportation review, 168, 102940 is available at https://doi.org/10.1016/j.tre.2022.102940.

A Patrol Routing Problem for Maritime Crime-Fighting

Abstract

In this study, we investigate a patrol routing problem for fighting maritime crime that is motivated by challenges faced in actual practice. Although maritime shipping and ecosystems are critical to human well-being, shipping lanes and related natural resources are vulnerable to maritime crimes. However, the time, location, and extent of the illegal activities in these areas are largely unknown, and maritime authorities have scant resources (such as patrol boats and aircraft) to monitor them. To tackle this challenge, we propose a novel approach to identify suspicious ships and develop patrol routing methods to enhance the patrol efficiency. The problem of enhancing patrol efficiency is analyzed in three scenarios that differ according to the availability of aerial photographs. We formulate three mathematical programming models to address this problem in each scenario. The patrol route is optimally designed based on information available online. Extensive numerical experiments are conducted to validate the effectiveness and efficiency of the proposed patrol routing models. Maritime illegal activities are attracting increasing attention, and our proposed approach can be applied to various maritime crime scenarios in oceans and seas around the world.

Keywords: maritime crime-fighting, patrol routing, selective traveling salesman problem, integer programming, maritime security.

© 2022. This manuscript version is made available under the CC-BY-NC-ND 4.0 license http://creativecommons.org/licenses/by-nc-nd/4.0/

1. Introduction

Crime at sea (e.g., illegal fishing, smuggling of banned animal products, and drugs) poses a serious threat to maritime shipping lanes and marine ecosystems, both of which are particularly vulnerable. For instance, according to the United Nations Food and Agriculture Organization, 34.2% of global fisheries have been fished beyond their sustainable limits (UNFAO, 2020). The World Wildlife Fund for Nature reports that the population of marine vertebratess decreased by almost half (49%) between 1970 and 2012 (WWF, 2015). Key factors contributing to this problem are overfishing and illegal fishing (MSC, 2022). Illegal (unregulated, or unreported) fishing threatens the sustainability of fish populations, ecosystems, and the livelihoods of those who fish legitimately, with the economic losses associated with illegal fishing estimated to be worth USD10–23.5 billion annually (MSC, 2022). In addition to illegal fishing, kidnapping, human trafficking, drug smuggling, and trade in banned animal products, such as rhino horn and ivory, are creating maritime security issues and have attracted the attention from maritime authorities (ICC, 2022; Nordling, 2017).

The most significant challenge in combating maritime crime is the contradiction between the shortage of physical resources available to monitor illegal activities and the vastness of the waters to be monitored. For example, South Africa (SF) reports that "the navy has only four frigates, three submarines, a handful of patrol vessels and aircraft to patrol this country's exclusive economic zone which exceeds its land area by 25%," which is equivalent to a country of 2.38 million km^2 using six police cars to patrol its entire territory (Nordling, 2017). Although there are abundant historical records describing the coastal poaching of high-value species (e.g., rock lobster and abalone) in SF, the extent of illegal fishing in SF's open oceans is largely unknown, indicating the likelihood that most transgressions go undetected (Nordling, 2017).

In the last decade, a number of countries have developed remote sensing systems to enhance the efficiency of maritime crime detection. For example, SF introduced a vessel-tracking system (VTS) that requires ships above a certain size to carry an automatic identification system (AIS) tracker. This VTS is capable of remotely tracking ships in real time and sending alerts to suspicious ships that enter SF's waters. Similar remote sensing systems

have been developed by countries such as the United States, Australia, and India (Nordling, 2017). Plans are also in place to use satellites equipped with high-resolution cameras or synthetic-aperture radar to collaborate with the AIS and detect ships that have deactivated their trackers (Nordling, 2017).

Compared with ships with operating AIS trackers, "dark" ships with deliberately deactivated AIS trackers are more likely to engage in crimes. However, it is much more difficult to detect these ships without obtaining additional information through other forms of detection. Although satellites carrying cameras or radar can provide essential information for detecting dark ships, the huge investment required to launch the satellites makes this approach impractical. Therefore, in some areas, it is more practical to collaborate with commercial airlines. For example, attaching cameras to planes that fly over marine reserves can facilitate the detection of any vessels that enter these sensitive areas. Figure 1 shows examples of aerial photographs (APs) which is obtained from Gallego et al. (2018). APs such as these can be transmitted to a ground station and used to detect suspicious ships, with any dark ships not detected by the AIS appearing in the APs. We refer to this innovative joint application of AIS and APs as the AIS-AP approach.

The ultimate goal of maritime crime-fighting is not simply to observe poachers or smugglers. Rather, maritime crime needs to be prevented in a timely fashion. Thus, the relevant maritime authorities need to dispatch patrol boats to specific maritime reserves and perform on-the-spot inspections, even when they have the support of AIS-AP. Some ships may simply lose their AIS tracker signal due to hardware or software failure, whereas others may deliberately engage in poaching or smuggling. To identify real, specific illegal activity, maritime inspectors need to board dark ships when they enter restricted waters.

Maritime patrols need to ascertain which suspicious ships they need to observe and inspect during a patrol. Because suspicious ships are not necessarily committing crimes, maritime inspectors have no option but to inspect as many ships as possible. Therefore, it is reasonable for maritime inspectors to use the number of inspected suspicious ships as a performance

indicator to measure the achievements of a patrol mission. More proficient maritime inspectors are able to observe and inspect a large number of suspicious ships each day.

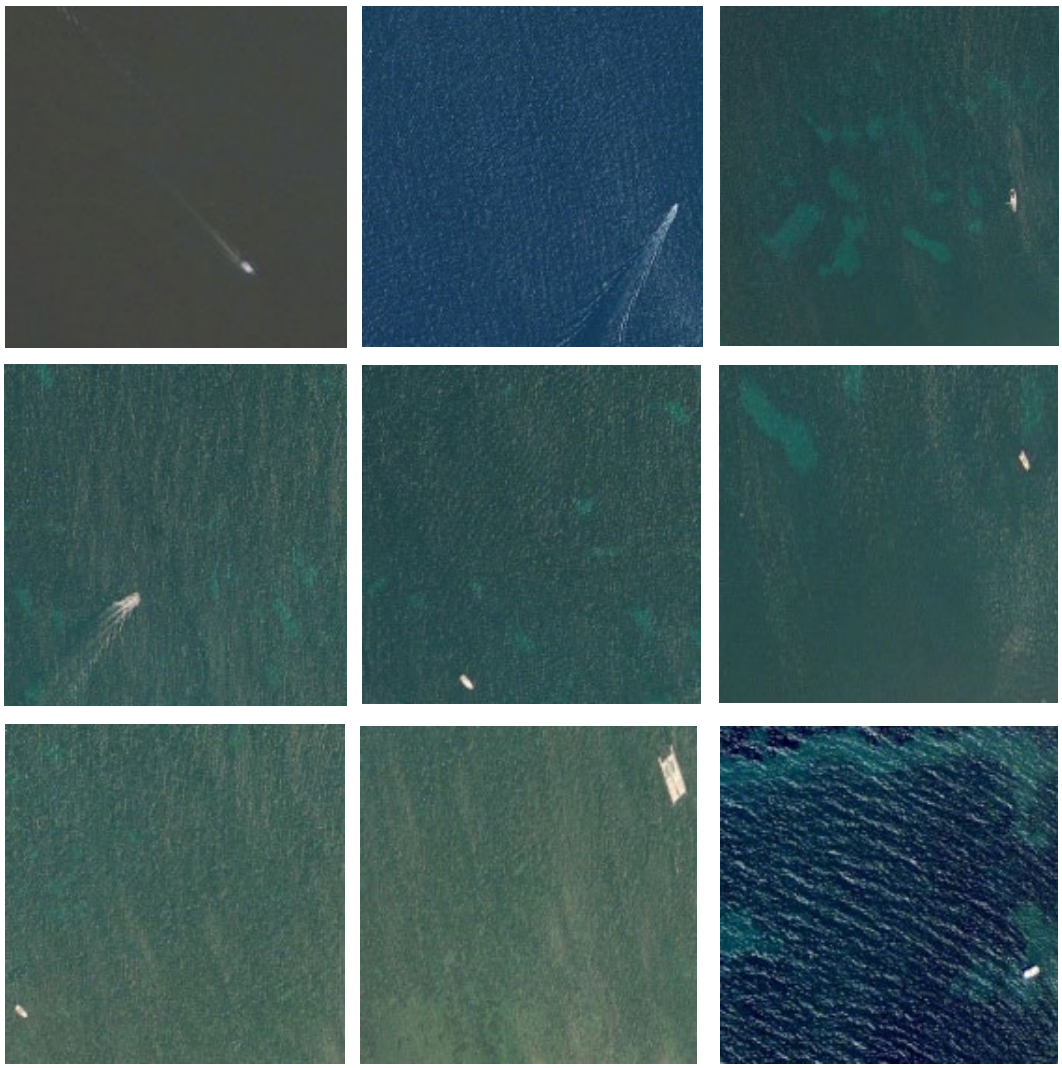

Figure 1 Some aerial photograph samples

Although numerous factors can affect the performance of a patrol (i.e., the number of suspicious ships inspected), patrol routing decisions undoubtedly play a crucial role in determining the outcomes of a patrol. Patrol routing essentially involves addressing two core sub-problems: learning the locations of suspicious ships and designing patrol routes. With the aid of AIS-AP, maritime inspectors are now able to determine the location of previously undetectable ships, which has significantly altered the routing problem and enhanced the patrol efficiency.

To evaluate the benefits of using AIS and APs for patrol routing, we consider three scenarios with and without the support of AIS-AP. In the first scenario (Scenario 1), we consider a situation in which the locations of suspicious ships are completely unknown. We can only assume the ships are randomly distributed throughout the maritime area, and patrol boats may encounter suspicious ships while on patrol. In the second scenario (Scenario 2), we consider a situation in which the AIS-AP approach is used to locate suspicious ships. In that scenario, the maritime inspectors need only to determine the necessary patrol route to inspect as many suspicious ships as possible, while considering the possible travel time and distance restrictions. Because APs generally do not cover the entire restricted areas, we also investigate a partial AIS-AP supported scenario that can be treated as a mix of Scenarios 1 and 2. The main difference between these scenarios is whether the inspectors are aware of a ship's location, which results in different modeling approaches.

The value of investigating the patrol routing problem with either the full or the partial support of AIS-AP is self-explanatory. Given the lack of available location information prior to the introduction of AIS-AP, it was difficult to set specific objectives for patrolling. In this respect, the introduction of AIS-AP has clarified the patrol objective by transforming the location of dark ships from a probability to a deterministic Boolean value. With accurate location information, maritime inspectors are no longer forced to conduct searches based on uncertain objectives, and thus their workload has been greatly reduced. This, in turn, has substantially enhanced the efficiency of maritime patrols. Patrol missions require much less travel distance and time to inspect the same number of suspicious ships or equivalently, to inspect more ships within the same travel time or distance. This improvement in patrol efficiency is even more valuable in light of the small number of patrol boats compared with the vastness of the waters to be monitored.

Although maritime security is a hot topic in maritime studies, most studies in this area focus on strategic, political, and empirical issues. The major topics include the ecosystem assessment (Frederiksen et al., 2021; Menegon et al., 2018), the relationship between the blue economy and maritime security (Voyer et al., 2018a; Voyer et al., 2018b), geopolitical

dimension (De Santo, 2020; Germond, 2015), regional maritime security investigation (Belhabib et al., 2019; Guilfoyle, 2019; Nordling, 2017; Okafor-Yarwood, 2020), law and maritime security (Guilfoyle, 2019; Ryan, 2019). For a comprehensive understanding of research on maritime security, refer to Bueger (2015) and Bueger and Edmunds (2017).

It should be noted that operational level research in this field attracts limited attention compared with the rich literature on strategic, political, and empirical studies. To the best of our knowledge, no studies focus on the maritime patrol routing problem. Some studies focus on the patrol routing problem on land. Table 1 summarizes the literature on land troopers patrol routing. These studies can be divided into two categories. The first category uses simulation-based methods to derive the patrol routes, e.g., Chen et al. (2017), Portugal and Rocha (2013), and Steil et al. (2011). Although their study background is more elaborated, the research results lack analytical insights. Another category of studies is developed from the vehicle routing problem. One pioneer study is Keskin et al. (2012) who established a mixed-integer linear programming model to determine optimal patrol routes of state troopers for maximum coverage of highway spots with high frequencies of crashes (hot spots). This formulation is similar to the team orienteering problem with time windows. The major difference is that Keskin et al. (2012) do not have a fixed "profit" associated with each location. Subsequent studies made extensions from different aspects. Dewil et al. (2015) reformulate Keskin et al. (2012)'s model as a minimum cost network flow problem and extend it to the multi-commodity minimum cost network flow model by considering several practical additions. Çapar et al. (2015) extend Keskin et al. (2012)'s model and demonstrate performance improvement through intensive instances. Li and Keskin (2014) extend Keskin et al. (2012)'s model to the scenario of multiperiod, bi-criteria, and joint optimization of dynamic location-routing decisions. Willemse and Joubert (2012) study the patrol routing problem from another aspect. They propose a min-max k postmen problem to the routing of security guards. Compared with land troopers, maritime police are responsible for vaster regions, which has implications for the design of patrol routing problems. The number of suspicious ships is much lower than that of hot spots in the road network. Little information can be obtained and utilized to locate the

position of suspicious ships, and limited resources (e.g., the number of patrol boats) can be invested to complete this mission. These characteristics require a novel approach and tailored models to address this problem. Routing is widely investigated in other transportation problems, such as drone-truck joint routing (Gonzalez-R et al., 2020; Zeng et al., 2022), liner shipping routing (Duan et al., 2021; Li et al., 2022; Zhen et al., 2020), vehicle routing (Bahrami et al., 2020; Basso et al., 2022; Gmira et al., 2021; Lin et al., 2021; Liu et al., 2021; Poon et al., 2022; Wang et al., 2020), as well as orbit and machine layout problem (Qi et al., 2022) to name a few. We enrich the literature by applying routing methods to the maritime patrol process.

Table 1 Summary of Literature on Patrol Routing

Paper	Problem and major considerations	Approach
Keskin et al. (2012)	Patrol routing; Maximum coverage; Team orienteering problem with time windows;	Local and tabu-search based heuristics
Chen et al. (2017)	Police patrols; Multi-agent patrol routing; Bayesian-based decision making; Online agent-based simulation	Ant colony algorithm
Portugal and Rocha (2013)	Multi-robot patrol; Fault-tolerance; Security	Greedy Bayesian strategy; State exchange Bayesian strategy
Dewil et al. (2015)	Minimum cost network flow problem; Multi-commodity;	Cplex
Li and Keskin (2014)	Bi-criteria; Multi-period; Dynamic location and routing problem;	ε-constraint approach; Cplex; Heuristic algorithm
Çapar et al. (2015)	Maximum coverage patrol routing; Multi-start routes; Diversion from patrols; Delay starting the shifts	Cplex
Willemse and Joubert (2012)	Chinese postman problem; Security guards routing; Continual patrolling; Arc Routing	Tabu search
Steil et al. (2011)	Nondeterministic patrol routing;	Simulation
Sun and Wang (2018)	Freeway service patrol; Route coverage and fleet allocation	Genetic algorithm; Simulated annealing
Jiang et al. (2022)	Patrol routing optimization; Smart city management; Road segment classification	Genetic algorithm
Saint-Guillain et al. (2021)	Partrol routing; Stochastic programming; On-demand transportation; Optimization under uncertainty; Recourse strategies	Recourse strategy; Expected cost computation
Sun et al. (2018)	Patrol routing; Fleet allocation on freeways; Overlapping/non-overlapping patrol	Genetic algorithm

Every moment, maritime crimes are taking place around the world, including but not limited to illegal fishing and harvesting, ocean dumping and discharge, illicit drug trafficking,

and other crimes (ICPO, 2019; UNODC, 2011, 2021). Areas such as Eastern and Southern Africa, the Indian Ocean region, the Gulf of Guinea, the Red Sea and the Gulf of Aden, and the Sulu and Celebes Seas are recognized hot-spots for maritime crime (ICPO, 2020, 2021a, b; Stable Seas, 2019). Therefore, our proposed patrol routing methods are applicable in a wide range of scenarios.

The remainder of this paper is organized as follows. Section 2 provides a detailed description of the considered problem and formulates three mathematical programming models for three specific scenarios in this problem. To validate the proposed models, we conduct two numerical experiments in Section 3. Conclusions are drawn in Section 4.

2. Problem statement

Maritime management authorities patrol given maritime regions to detect suspicious ships and identify maritime crimes. To focus on the major objective of our problem, we make the following assumptions:

a) The given maritime region to be inspected is a rectangular area. Without loss of generality, the length of the horizontal side of the region is no smaller than that of its vertical side.
b) Only one patrol boat is assigned to fulfill the inspection mission in a given maritime region.
c) The speed and range/voyage of the patrol boat are given and constant.
d) The patrol boat can discover and identify illegal ships within the given latitudinal and longitudinal range of the patrol route. Therefore, the vessel inpsects a belt/band region on the patrol route.
e) The patrol route is a loop.
f) Not every part of the maritime district can be inspected by the patrol boat because of the limitations on the travel distance and/or time.
g) The fuel consumption during onboard inspections is not considered.

The objective of the problem is to maximize the number of suspicious ships inspected. In Scenario 1, because the locations of suspicious ships are unknown, we formulate the problem

as maximizing the expected number of ships inspected. We adopt a simple serpentine/switchback route pattern. A mixed-integer nonlinear model is built to optimize the route configuration. In Scenario 2, with the help of AIS-AP, the locations of suspicious ships can be identified. In this case, our objective is to inspect as many suspicious ships as possible. Scenario 3 combines Scenarios 1 and 2, so we maximize the summation of the number of inspected suspicious ships in the AP-covered region and the expected number of suspicious ships inspected in the regions without AP coverage.

2.1. Notation

The notation for describing the following models is listed in Table 2.

Table 2 Notation

Sets	
A	Set of links
V	Set of nodes
V^+	Set of nodes including origin and dummy origin
Vr	Set of nodes in region r
$\overline{V}_r$	Set of boundary nodes in region r
V_0	Set of nodes (location identified)
Indices	
i	Index of node
j	Index of node
s	Depot
t	Depot replica
r	Index of region
Parameters	
b	Inspection scope of patrol boat
c	Area covered by the study water region
c_r	Area covered by region r
d_{ij}	Travel distance between i and j
q	Weighted parameter derived from historical records
q_r	Weighted parameter derived from historical records in region r
l_h	Horizontal length of patrol region
lv	Vertical length of patrol region
l_0	Maximum traveling range of patrol boat

Decision Variables	
$\bar{l}$	Total length of patrol route in Scenario 1
n	Number of switchback segments in Scenario 1
x	Unit length of horizontal link in Scenario 1
y	Unit length of vertical link in Scenario 1
l	Patrol route in Scenario 1
u_{ij}	A binary variable to indicate whether node i is followed by node j in Scenarios 2 or 3
v_i	A binary variable to indicate whether node i is selected in Scenarios 2 or 3
w_i	Sequence/position of node i in the route l

2.2. Basic scenario

We first consider the basic scenario without the support of AIS-AP (Scenario 1). In this scenario, the extent of illegal activities is largely unknown (Nordling, 2017). Suspicious ships may be located in any part of the marine protected area. A patrol boat should inspect the whole area, rather than several identified hotspots. Therefore, we set the objective in this scenario as maximizing the expected number of suspicious ships inspected. We assume that the suspicious ships are randomly distributed in the maritime district. Accordingly, it is important to design a patrol route l to maximize the likelihood of discovering suspicious ships, i.e., maximizing the detection band coverage of the route. In this case, owing to the lack of prior information, the patrol boat is expected to inspect the whole area. Therefore, in the first scenario, we consider a simple route pattern/structure, i.e., a serpentine/switchback patrol route, as shown in Figure 2. This route is easy to execute and can cover the entire region in a roughly even manner. We then propose a model to optimize the parameters of this route structure.

To begin with, the patrol route is assembled by a set of horizontal and vertical links. Take Figure 2 for example, the horizontal links involve links a_1, a_3, a_5, a_7, and a_9, and the vertical links involve links a_2, a_4, a_6, a_8, and a_{10}. The horizontal links can be further classified into three sub-categories according to their length: (i) initial horizontal link a_1 whose length is x; (ii) horizontal links whose length is $2x$, such as a_3, a_5, and a_7; (iii) last horizontal link a_9 whose length is the sum of links in the second sub-category. Similarly, the vertical links can also be classified into three sub-categories: (iv) vertical links whose length is y, such as a_2, a_4, and a_6;

(v) last vertical link a_{10} whose length is $2x$; (vi) second-last vertical link a_8 whose length is $2x+y$.

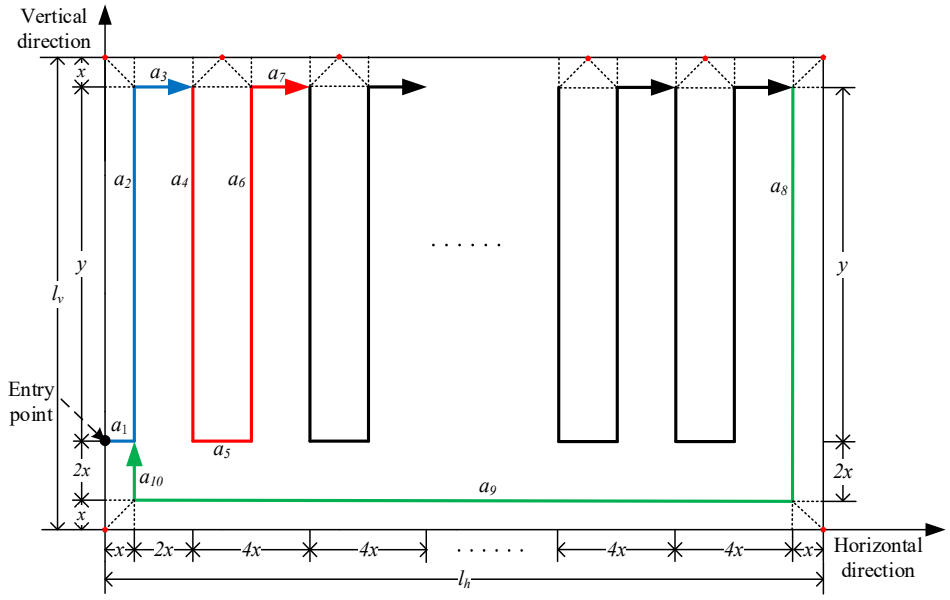

Figure 2 Basic structure of patrol route in the scenario without the support of AIS

The patrol boat inspects the maritime region in the following sequence. It goes along the entry channel a_1 to enter the inspection area. Then, after the initial entry procedure, it turns a corner and goes along the link a_2. When it approaches the boundary of the water district, it turns to the horizontal direction and goes along the link a_3. Links a_1, a_2 and a_3 form the route segment s_1, which is a common component for each potential patrol route. Then, the patrol boat enters the next segment s_2 which is a switchback segment and is shown by red/black color. s_2 is a flexible component of the patrol route and consists of links a_4, a_5, a_6, and a_7. The number of s_2 depends on the specific situations. The patrol boat could repeatedly use this segment to build the patrol route and cover the whole area. When the patrol boat approaches the other side of the maritime region, it turns into the route segment s_3 (shown by green color) and enters the return procedure. The patrol boat sequentially goes along the links a_8, a_9, a_{10}, returns to the entry channel a_1, and then leaves the maritime region.

In summary, the whole patrol route consists of three types of route segments: Entry segments s_1, switchback segment s_2, and return segments s_3. This structure is extendable to a

variety of patrol routes by assembling and modifying the three modules, as shown in Figure 3. The grey belt in Figure 3 reflects the patrol boat's inspection scope. Note that the patrol route can be adjusted, e.g., move along horizontal and vertical directions or extend/shorten the certain link's length, task by task to inspect every spot of the water district.

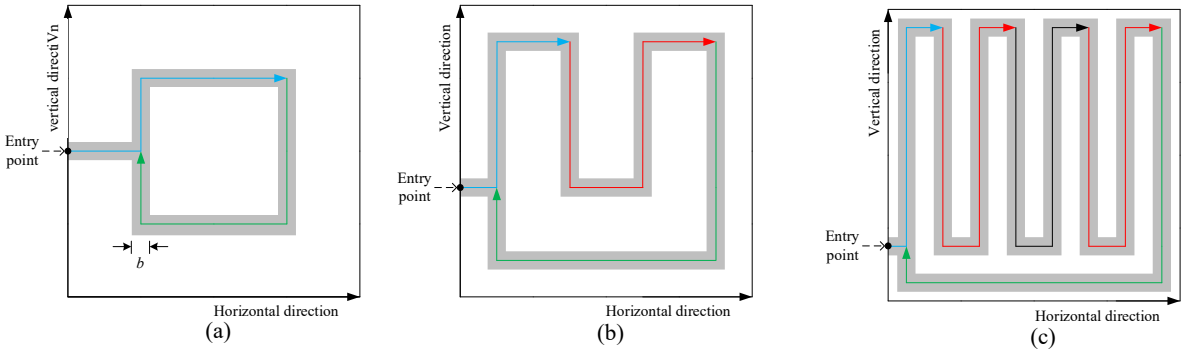

Figure 3 Some specific switchback patrol routes

Note that this route structure is a special case of the swath path (Daganzo, 1984), which shows the swath path is near-optimal solution for the traveling salesman problem in zones of different shapes. Numerical studies show that the gap between the swath path and the optimal solution is within 5%.

Since the location of suspicious ships is uncertain, a weighted parameter is needed to represent the potential of capturing and inspecting suspicious ships. Let b denote the inspection scope of patrol boat (the breadth of inspection belt as shown in Figure 3), η denote the average number of inspected suspicious ships every day in the given water district in history and c denote the area covered by the entire water district. The weighted parameter can be expressed as $q = b \cdot \eta / c$. Let $\bar{l}$ denote the total length of patrol route l. The specific problem can be simply formulated as:

[M1] $$\max \ q\bar{l} \tag{1}$$

subject to

$$4x + 4n \cdot x = l_h \tag{2}$$

$$4x + y = l_v \tag{3}$$

$$\bar{l} = (x+y+2x) + n(2y+4x) + ((y+2x) + (4n \cdot x + 2x) + 2x+x) \quad (4)$$

$$\bar{l} \le l_0 \quad (5)$$

$$x \ge \frac{b}{2} \quad (6)$$

$$x, y > 0, n \in \not\in . \quad (7)$$

Objective (1) maximizes the covered area which subsequently maximizes the likelihood of inspecting suspicious ships. Eq. (2) means the sum of horizontal length of patrol route (projection on the horizontal direction) and its margins to both sides equals the region's horizontal side length l_h. Eq. (3) requires the sum of vertical length of patrol route (projection on the vertical direction) and its margins to both sides equals the reegion's vertical side length l_v. An illustration of Eq. (2) and Eq. (3) are shown in Figure 2. Eq. (4) defines the total length of patrol route l. As illustrated in Figure 2, the right term of Eq. (4) is the summation of the length of route segments s_1 (a_1, a_2, a_3), s_2 (a_4, a_5, a_6, a_7),…, s_2,…, and s_3 (a_8, a_9, a_{10}, a_1). Eq. (5) requires the patrol route length $\bar{l}$ should be no larger than the patrol boat's voyage/range l_0. Eq. (6) prevents inspection belts overlap. Eq. (7) defines the domain of variables. [M1] is a mixed-integer nonlinear programming model but can be easily solved by enumerating n from 0, 1, 2, …, and terminating when the constraints no longer hold. Detailed steps of the solution method are presented as follows:

Algorithm for [M1]	
1	Set $n \leftarrow 0$.
2	Given n, calculate x by Eq. (2).
3	Given n and x, calculate y by Eq. (3).
4	Given n, x, and y, calculate $\bar{l}$ by Eq. (4).
5	If constraints (5) and (6) are satisfied, $n \leftarrow n + 1$ and go to Step 2. Otherwise, stop.

2.3. AIS-AP aided scenario

In this section, we consider the extended scenario with the support of AIS-AP (Scenario 2). The AIS could identify the location of ships that are willing to provide their locations, while the APs could identify the location of all ships, no matter they are willing to or not. By matching

the ships in both AIS and AP systems, the dark ships can be identified. In this section, we make the following assumption:

h) The air view provided by the airlines can identify the majority of suspicious ships.

Assumption h) implies that the air view taken by airlines can cover the whole area of the maritime region. Then, the maritime inspectors just need to design a patrol route l to visit these identified locations and inspect these suspicious ships. Considering the constraint of travel time/distance, not every suspicious ship can be visited. Therefore, the patrol route l should visit as many suspicious ships as possible. In this section, we build an AIS-AP joint aided patrol routing (AAPR) model to address this problem.

Given an undirected graph $G(V^+, A)$, where V^+ denotes the set of nodes and A denotes the set of links. $V^+ = V \cup \{s, t\}$ includes a set of target sites V and one depot s with its replica t. V represents the locations of suspicious ships. A patrol boat departs from the depot s, visits the selected sites (to be determined) to inspect the suspicious ships, and then returns to the depot t. A link $(i, j) \in A$ is the traveling leg between node $i \in V \cup \{s\}$ and node $j \in V \cup \{t\}$, $i \neq j$. The travel distance of link (i, j) is denoted as d_{ij}. The total travel distance should be no longer than the maximum traveling range l_0. Let u_{ij} denote a binary variable to indicate whether node i is followed by node j in the route l, v_i denote a binary variable to indicate whether node i is selected and w_i denote the position of node i in the route l (the depot s is the first node). The objective can be represented as $\sum_{i \in V} v_i$. Then, the AAPR model can be formulated as

[M2]
$$\max \sum_{i \in V} v_i \tag{8}$$

subject to

$$\sum_{j \in V \cup \{t\}} u_{sj} = \sum_{i \in V \cup \{s\}} u_{it} = v_s = v_t = 1 \tag{9}$$

$$\sum_{i \in V \cup \{s\}} u_{ik} = \sum_{j \in V \cup \{t\}} u_{kj} = v_k, \forall k \in V \tag{10}$$

$$\sum_{i \in V \cup \{s\}} \sum_{j \in V \cup \{t\}} d_{ij} u_{ij} \leq l_0 \tag{11}$$

$$2 \leq w_i \leq |V| + 2, \forall i \in V \cup \{t\} \tag{12}$$

$$w_i - w_j + 1 \le \left(|V|+1\right)\left(1-u_{ij}\right), \forall i, j \in V \cup \{t\}, i \ne j \quad (13)$$

$$u_{ij} \in \{0,1\}, \forall i \in V \cup \{s\}, j \in V \cup \{t\}, i \ne j \quad (14)$$

$$v_i \in \{0,1\}, \forall i \in V \quad (15)$$

$$w_i \in \mathbb{Z}^+, \forall i \in V. \quad (16)$$

Objective (8) aims to maximize the total number of inspected suspicious ships. Constraints (9) ensure that the patrol route *l* start at the depot *s* and return to the depot (i.e., replica *t*) after finishing inspection. Constraints (10) ensure the connectivity of the patrol route, and each selected inspection site can only be visited once. Constraint (11) defines the total travel distance limitation. Constraints (12) and (13) prevent the subtours (Miller et al., 1960; Zhang et al., 2020). Constraints (14)–(16) define the domains of decision variables. Note that [M2] is essentially an application of the traveling salesman problem with profits (Vidal et al., 2016), namely selective traveling salesman problem (Laporte and Martello, 1990).

2.4. Partial AIS-AP aided scenario

In this section, we consider the scenario that the planes' fly routes could only cover a part of the maritime region, and discover a few dark ships (Scenario 3). Essentially, this scenario can be considered as a blend of the basic scenario presented in Section 1.1 and the extended scenario presented in Section 1.2. For the sake of completeness, we make the following assumption

i) The air view provided by the airlines could only identify a limited number of suspicious ships.

Note that incomplete AP information described by Assumption i) is still useful since it can help the maritime inspectors eliminate the region already covered by APs and then narrow the area they have to patrol without knowing the targets. As shown in Figure 4, the red lines represent the air routes that pass through the maritime region, and the grey belts represent the area covered by the photographs taken from the airborne camera. The whole area is divided

into several regions. In blank regions, the location of suspicious ships is unknown, while in grey belts, the suspicious ships can be photographed and identified. That implies different patrol strategies should be adopted to deal with different water regions. In blank regions, the patrol boat needs to cover as much area as possible. Meanwhile, in grey regions, the patrol boat just needs to investigate as many locations of suspicious ships as possible. Therefore, in this section, we build a new model to address the routing problem in this scenario.

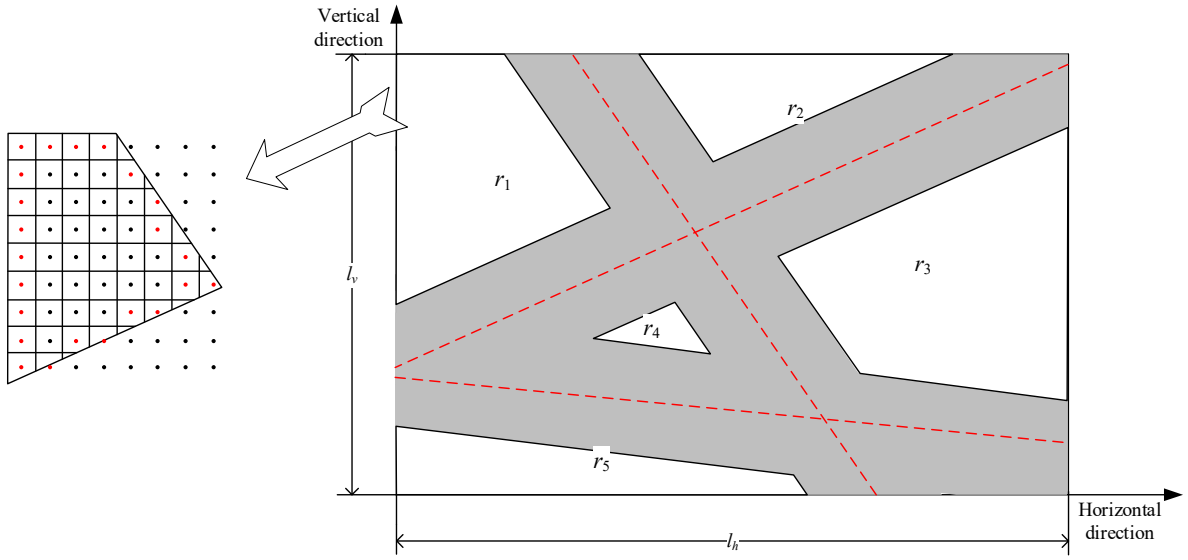

Figure 4 An illustration of Scenario 3

It is easy to see that the blank district is divided into several independent regions. The whole district composed of these independent regions is non-convex. The objective function cannot be easily represented by a closed-form function. Therefore, we provide here an approximation method toward an integer programming model. We discretize the water regions to be inspected by a set of polygons (most of which are squares). Each polygon is represented by a representative spot/node in it. For example, in Figure 4, the region r_1 is discretized by a set of square polygons and represented by a set of centroids. The side length of polygons should be larger than the inspection scope of a patrol boat (i.e., the breadth of grey belts as illustrated in Figure 3), because small polygons make the scanning/inspection belts overlap, and the overlapping areas provide no additional information. The set of representative nodes in region

r_1 is denoted as V_1. The patrol boat should select some of these polygons, and then design a route to visit them.

In addition, the patrol route in blank regions should not cross itself, since the crossed route segments also make the scanning/inspection belts overlap, and thus, the overlapping areas provide no additional information. Therefore, in this study, we design a rule to prevent this issue. Specifically, we require that the selected polygons should be neighboring with each other, and the patrol boat should visit these neighboring polygons step by step. In other words, the behavior that skipping the neighboring polygon and directly visiting other enclaves (i.e., polygons do not share a border) is not allowed. Figure 5 further illustrates this rule by taking region r_1 (shown in Figure 4) as an example. Figure 5 (a) shows that a representative route segment in r_1 that its component links only connect their neighboring polygons. Combing with the requirement that each selected node should be visited only once, the link-crossing situation presented in Figure 5 (b) can be prevented.

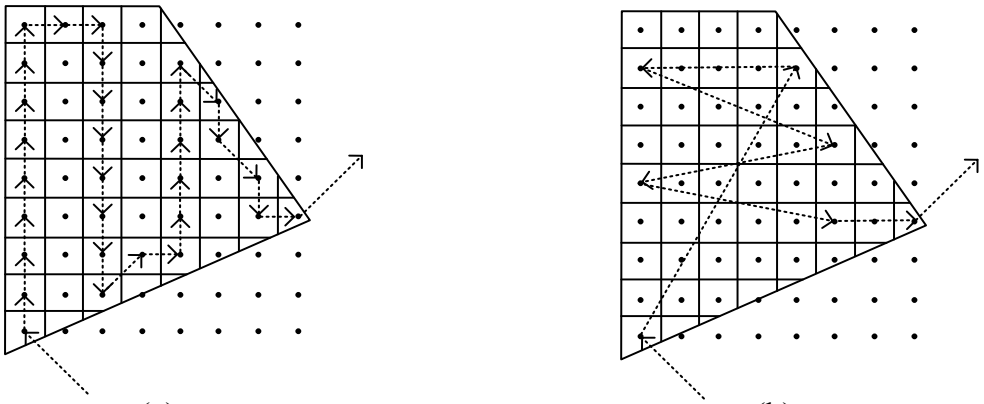

Figure 5 An illustration of the rule to prevent route overlap

Since the specific location of suspicious ships is unknown in blank regions, a weighted parameter q_r should be attached to the route segment in each blank water region r to indicate the potential of capturing suspicious ships. Such a weight can be determined according to the historical patrol records, i.e., $q_r = b\eta_r/c_r$ where η_r and c_r are related to historical inspection records in region r: η_r denotes the average number of captured illegal ships and

c_r denotes the area covered by the inspection belt in region *r*. Then, q_r can be taken as a multiplier w.r.t. the length of route segment in region *r*.

Let *r* denote the index of a blank region, and *R* denote the set of *r*. Then, the representative node set in region *r* can be denoted as V_r. The length of route segment in blank region *r* can be expressed as the sum of its links $\sum_{i\epsilon V_r}\sum_{j\epsilon V_r} d_{ij}u_{ij}$, where d_{ij} is the length of link (i, j) and u_{ij} is the binary decision variable to indicate whether link (i, j) is selected. Let V_r^i denote the set of neighboring nodes of node $i \in V_r$ $\left(V_r^i \subseteq V_r\right)$, $\overline{V_r}$ denote the boundary nodes of region *r* (i.e., red nodes as illustrated in Figure 4), $\overline{V} = \{\overline{V_r}, r\epsilon R\}$ denote the boundary nodes of all regions, and V_0 denote the location set of identified suspicious ships. Then, [M2] can be extended to address the routing problem in this scenario.

[M3] $$\max \sum_{k\in V_0} v_k + \sum_{r\in R} q_r \sum_{i\in V_r}\sum_{j\in V_r} d_{ij}u_{ij} \tag{17}$$

subject to

$$\sum_{j\in V\cup\{t\}} u_{sj} = \sum_{i\in V\cup\{s\}} u_{it} = v_s = v_t = 1 \tag{18}$$

$$\sum_{i\in V_0\cup\{s\}\cup\overline{V}} u_{ik} = \sum_{j\in V_0\cup\{t\}\cup\overline{V}} u_{kj} = v_k, \forall k \in V_0 \tag{19}$$

$$\sum_{i\in V_r^m} u_{im} = \sum_{j\in V_r^m} u_{mj} = v_m, \forall m \in V_r \setminus \overline{V}_r, r \in R \tag{20}$$

$$\sum_{i\in V_r^m\cup V_0\cup\{s\}\cup_{r'\in R\setminus\{r\}}\overline{V}_{r'}} u_{im} = \sum_{j\in V_r^m\cup V_0\cup\{t\}\cup_{r'\in R\setminus\{r\}}\overline{V}_{r'}} u_{mj} = v_m, \forall m \in \overline{V}_r, r \in R \tag{21}$$

$$\sum_{i\in V\cup\{s\}}\sum_{j\in V\cup\{t\}} d_{ij}u_{ij} \le l_0 \tag{22}$$

$$2 \le w_i \le |V| + 2, \forall i \in V\cup\{t\} \tag{23}$$

$$w_i - w_j + 1 \le (|V|+1)(1-u_{ij}), \forall i, j \in V\cup\{t\}, i \ne j \tag{24}$$

$$u_{ij} \in \{0,1\}, \forall i \in V\cup\{s\}, j \in V\cup\{t\}, i \ne j \tag{25}$$

$$v_i \in \{0,1\}, \forall i \in V \tag{26}$$

$$w_i \in \mathbb{Z}^+, \forall i \in V. \tag{27}$$

Objective (17) aims to simultaneously maximize the number of visiting nodes (i.e., location of suspicious ships) in area covered by APs and the likelihood of capturing suspicious ships in

blank regions. Constraints (18) impose the patrol boat to start at the depot *s* and to return to the depot (i.e., replica *t*). Constraints (19)–(21) ensure the connectivity of the patrol route, and each selected inspection site can only be visited once. Constraints (19) allow the patrol boat to visit both the chosen nodes in V_0 and the chosen boundary node in $\bar{V}$. Constrains (20) allow the patrol boat in the interior region *r* to visit the neighboring nodes. Constrains (21) allow the patrol boat at the boundary of region *r* to visit the interior neighboring nodes, the depot, and the other regions. Constraint (22) concerns the patrol boat's travel distance limitation. Constraints (23) and (24) eliminate the subtours. Constraints (25)–(27) define the domains of decision variables.

3. Numerical studies

In this section, we perform extensive numerical experiments to demonstrate the applicability and effectiveness of the proposed model. The experiments are performed based on an illustrative and a large-scale instance with different input parameters. The experiments are coded in Python calling Gurobi of version 9.5.2 and implemented on a computer with AMD 8 Cores 2.9 GHz central processing unit and 16GB RAM.

Note that in all three scenarios, the overall objective is to inspect as many suspicious ships as possible. To better illustrate the comparison, the three models are applied to the same task (i.e., determining the numbers and locations of suspicious ships) and their performance is compared.

3.1. An illustrative instance

We first examine an illustrative example of a small area to demonstrate the applicability of the proposed models.

3.1.1. Description of parameters

As shown in Figure 6, *R* is an 80×50 km^2 region. Suppose that there are 10 suspicious ships in this region. The spots plotted in Figure 6 represent these suspicious ships. In Scenario 1, the geographical locations of the ships are unknown. The patrol boat follows the serpentine-style

path in performing its monitoring task. The inspection radius is assumed to be 5 km. Both sides of the patrol boat are monitored, and thus the inspection scope b is $5 \times 2 = 10$ km. In Scenario 2 , the locations of suspicious ships are identified via AIS-AP as shown in Figure 7 (a). Therefore, the patrol boat only needs to perform an on-the-spot investigation. Figure 7 (b) shows Scenario 3, in which the inspection area is divided into two regions. The light-colored region R_1 is covered by the AP, whereas the dark region R_2 is not covered. R_2 is an equilateral right triangular region measuring 1250 km^2. The patrol speed is 30 knots. The upper limit of patrol time is 4 hours and the corresponding upper bound of the patrol distance is 222.24 km. To obtain the average number of inspected illegal ships, we conduct several randomized experiments and find that the average value is 3. The weighted parameter q_2 is calculated as $\frac{10\times3}{1250} = 0.024$.

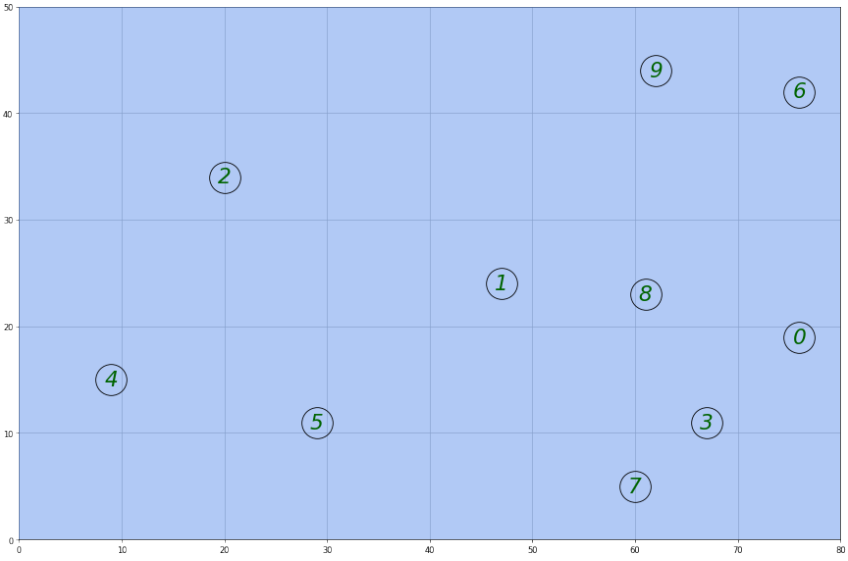

Figure 6 Scenario 1 in the illustrative instance

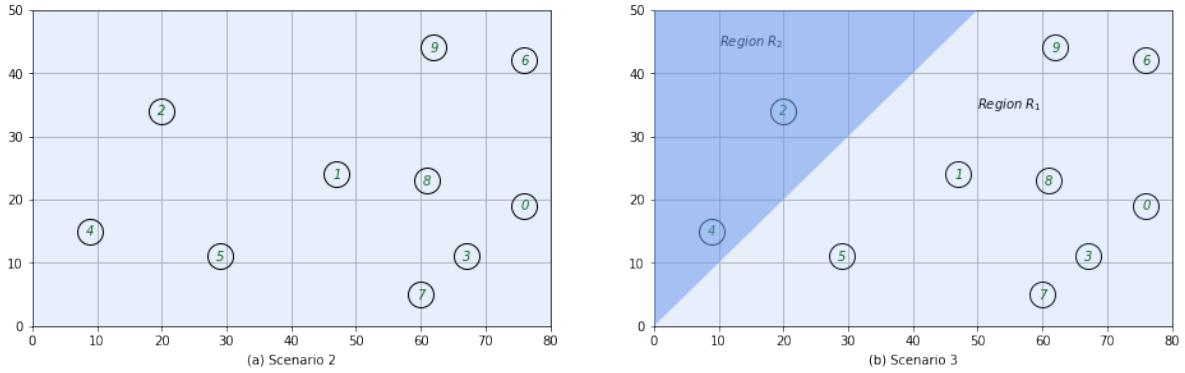

Figure 7 Scenarios 2 and 3 in the illustrative instance

3.1.2. Result analysis

We first solve [M1] to obtain the patrol route in Scenario 1. As shown in Figure 8, without the support of AIS-AP, the patrol boat follows a serpentine style path. The red solid line represents the patrol trajectory. The blue dotted line depicts the boundary of the inspection belt. The suspicious ships within this belt are observed and investigated, whereas the ships outside the belt escape inspection. The corresponding travel distance in this scenario is 220 km, which is close to the upper bound. However, 50% of the suspicious ships remain undetected, i.e., spots 0, 1, 2, 6, and 8.

We then examine Scenario 2. As shown in Figure 9 (a), the specific locations of the suspicious ships are known and the patrol boat needs only to determine the shortest route to visit these nodes, i.e., the loop represented by solid red lines. The total distance traveled is 209 km, similar to the distance traveled in Scenario 1. However, in this case, the inspection efficiency is different. In Scenario 2, all of the suspicious ships can be inspected, whereas in Scenario 1, only 50% of the ships can be investigated. Scenario 3 is a more general situation than Scenarios 1 and 2. One part of the region, i.e., Region R_2, is not covered by the Aps, and the locations of the suspicious ships in this region are not known. Therefore, we solve [M3] to obtain the optimal solution. The resulting optimal path is drawn in Figure 9 (b). The total distance traveled is 213 km. Note that owning to the distance limitation, not all suspicious ships and regions can be investigated. In this example, two suspicious ships, spots 4 and 5, escape investigation. In other words, 80% of the suspicious ships can be investigated in Scenario 3.

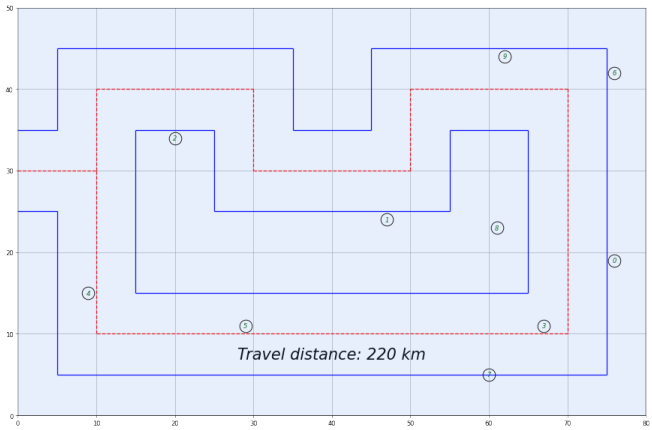

Figure 8 Patrol route in Scenario 1

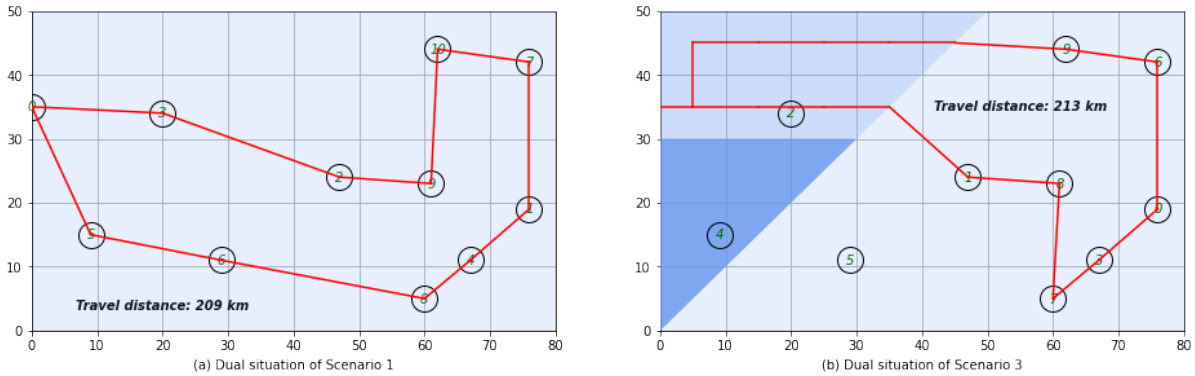

Figure 9 Patrol route in Scenarios 2 and 3

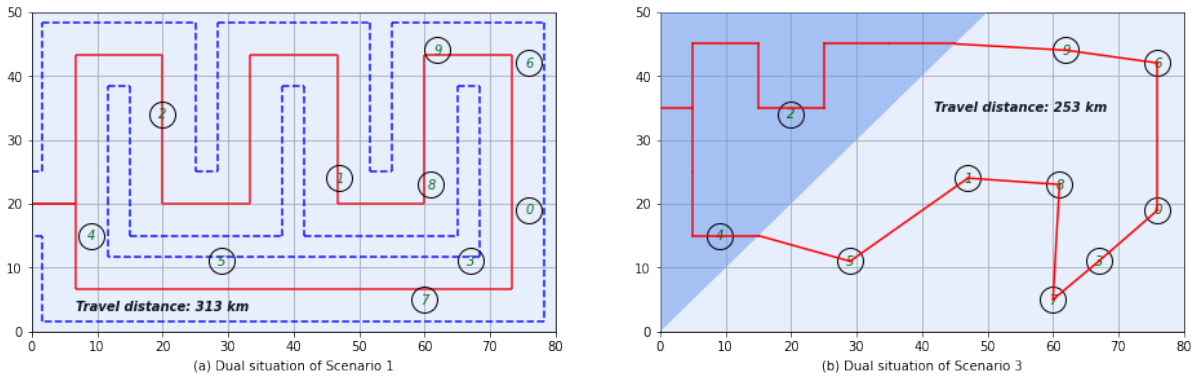

Figure 10 Dual situation of Scenarios 1 and 3

To further explore this problem, we examine a dual situation in where the objective is to determine the shortest route to inspect all potential nodes. Here, we use a trial-and-error procedure. Specifically, we iteratively increase the travel distance limitation to obtain different patrol routes. We then select the shortest patrol route that is capable of inspecting all potential nodes. The results are shown in Figure 10. If we want to investigate every suspicious ships, the patrol boat needs to travel at least 313 km in Scenario 1 and 253 km in Scenario 3. Without the support of AIS-AP, significant increases in travel distance are required to increase the numbers of suspicious ships investigated. These findings demonstrate that the proposed patrol routing model has the potential to significantly improve patrol efficiency.

3.2. A large instance

In this section, we further examine the effectiveness of the proposed patrolling approach in a large setting. To make our case study more realistic and comprehensive, we searched relevant public websites on maritime crimes, namely https://spyglass.fish/ and https://www.icc-ccs.org/.

The first website focuses on fishery-related crimes, and the second website reports piracy-related crimes. The records of fisheries-related crime, as well as other transnational crimes such as transshipment crimes and drug and arms smuggling, cover 2000 to 2020. The typical hot spots for illegal fishing are the Gulf of Guinea, Southeast Asia, and Indonesia. For instance, 370 fisheries-related crimes were reported in the Gulf of Guinea during the study period. The International Chamber of Commerce also lists the Gulf of Guinea as a hotspot for piracy. Globally, 135 crew members were kidnapped from their vessels in 2020, with the Gulf of Guinea accounting for over 95% of the kidnappings (ICC, 2022). In 2020, a record number of 130 crew members were kidnapped in 22 separate incidents (ICC, 2022). Overall, on average, 40 illegal fishing and piracy offenses are reported per year in this area, i.e., approximately 0.1 incidents per day.

We use public information to generate our case study scenario. As shown in Figure 11, the inspection region is a 150×100 km^2 area and 15 suspicious ships are detected in this instance. The yellow vertical line with "x"-type markers represents the coast line, and the red node represents the patrol boat depot. Given that only a limited number of suspicious ships enter this area at any given time (because otherwise the authorities would have deployed more resources and implemented stricter measures to govern the area), we believe that it is reasonable to assume that 15 suspicious ships are within the study region. Figure 12 shows a specific situation in Scenario 3 in which four airlines cover the region and divide the area into several parts. The other parameters remain the same as in the previous cases. The suspicious ships are randomly distributed within the study area. Because the required travel distance in Scenario 1 is much longer than the distances in Scenarios 2 and 3, we focus on the latter two scenarios.

We first examine the optimal patrol routes in Scenarios 2 and 3 using different performance requirements. We then solve [M2] to obtain the optimal patrol routes. Figure 13 shows the shortest patrol routes in Scenario 2 with different numbers of selected spots (i.e., suspicious ships). [M2] maximizes the number of visiting nodes.

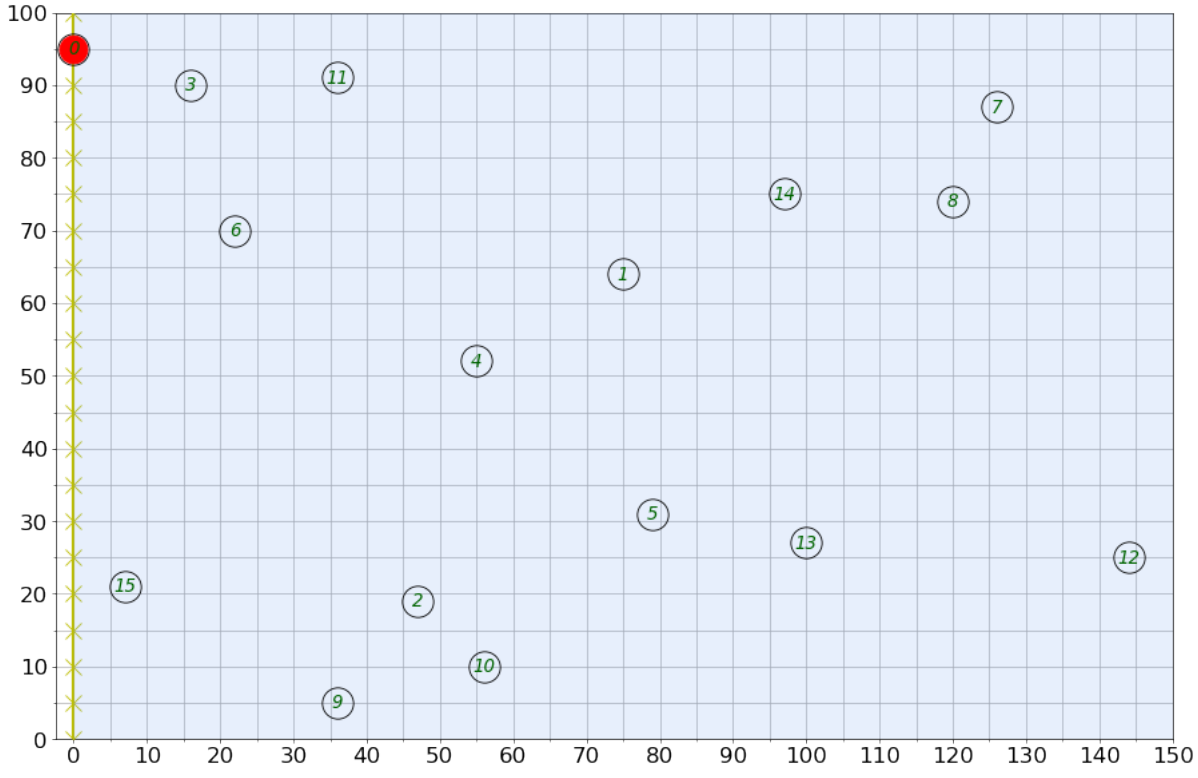

Figure 11 The locations of suspicious ships in the large instance

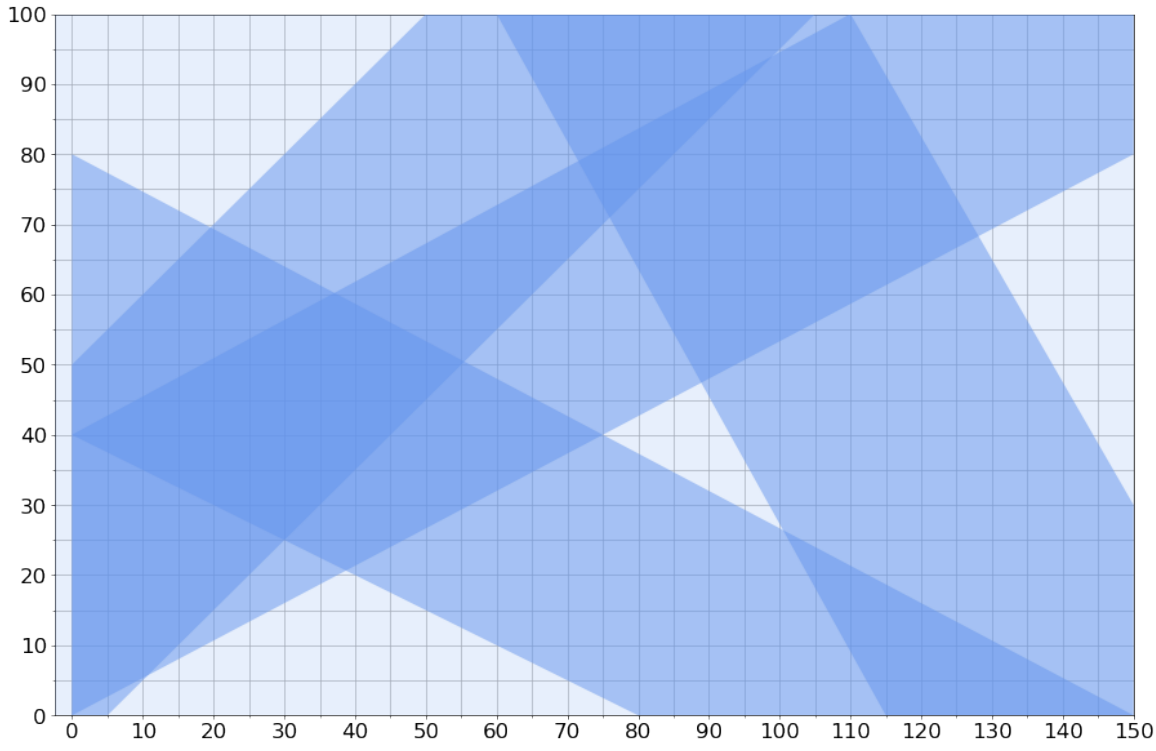

Figure 12 The area covered by AP in Scenario 3 in the large instance

Similarly, Figure 14 shows the shortest patrol routes with the different requirements in Scenario 3. In this scenario, the locations of the suspicious ships in the area not covered by APs

498 are unknown and thus the ships may not be detected. In this case, to increase the likelihood of
499 detecting the suspicious ships, we need to increase the patrol distance. Thus, Scenario 3
500 requires a much longer patrol distance than in Scenario 2 to visit the same number of suspicious
501 ships.

502 Figure 15 compares the patrol distances required in Scenarios 2 and 3. The horizontal axis
503 represents the numbers of nodes, which vary from 7 to 16. The vertical axis represents the
504 minimal travel distance needed to investigate these nodes. In Scenario 2, the minimal travel
505 distance is monotonously increasing with the number of nodes. However, in Scenario 3, this
506 monotonicity is not necessarily held. As shown in Figure 15, the travel distance needed to visit
507 9 nodes is longer than the travel distance for visiting 10 nodes. Given that the locations of the
508 suspicious ships are unknown, this phenomenon is not surprising. Another finding is that the
509 minimal travel distance in Scenario 3 increases faster than in Scenario 2. When visiting 7 nodes,
510 the difference in distance is 33 km, whereas the difference increases to 160 km when visiting
511 16 nodes. This phenomenon indicates the importance of AIS-AP.

512 To investigate how knowledge of the suspicious ship locations affects the performance,
513 we generate another three scenarios. Retaining the setting of 15 suspicious ships randomly
514 distributed in the study area, we add four different travel distance requirements, i.e., 200, 300,
515 400, and 500 km to Scenarios 2 and 3. The numbers of inspected ships are reported separately
516 in Table 3 for Scenarios 2 and 3. The column labeled “Gap” shows the difference between the
517 two scenarios. We can see all of the suspicious ships can be inspected within the travel limit of
518 500 km in all instances in Scenario 2, while this performance is not achieved in any instance
519 in Scenario 3. In addition, if the travel distance is not sufficient for the patrol boat to visit all
520 ships under both scenarios, the gap between Scenarios 2 and 3 tends to monotonically increase
521 with respect to travel distance. This phenomenon is consistent with the trend shown in Figure
522 15. These results further demonstrate the value of the AIS-AP information for optimizing the
523 patrol routes in maritime areas.

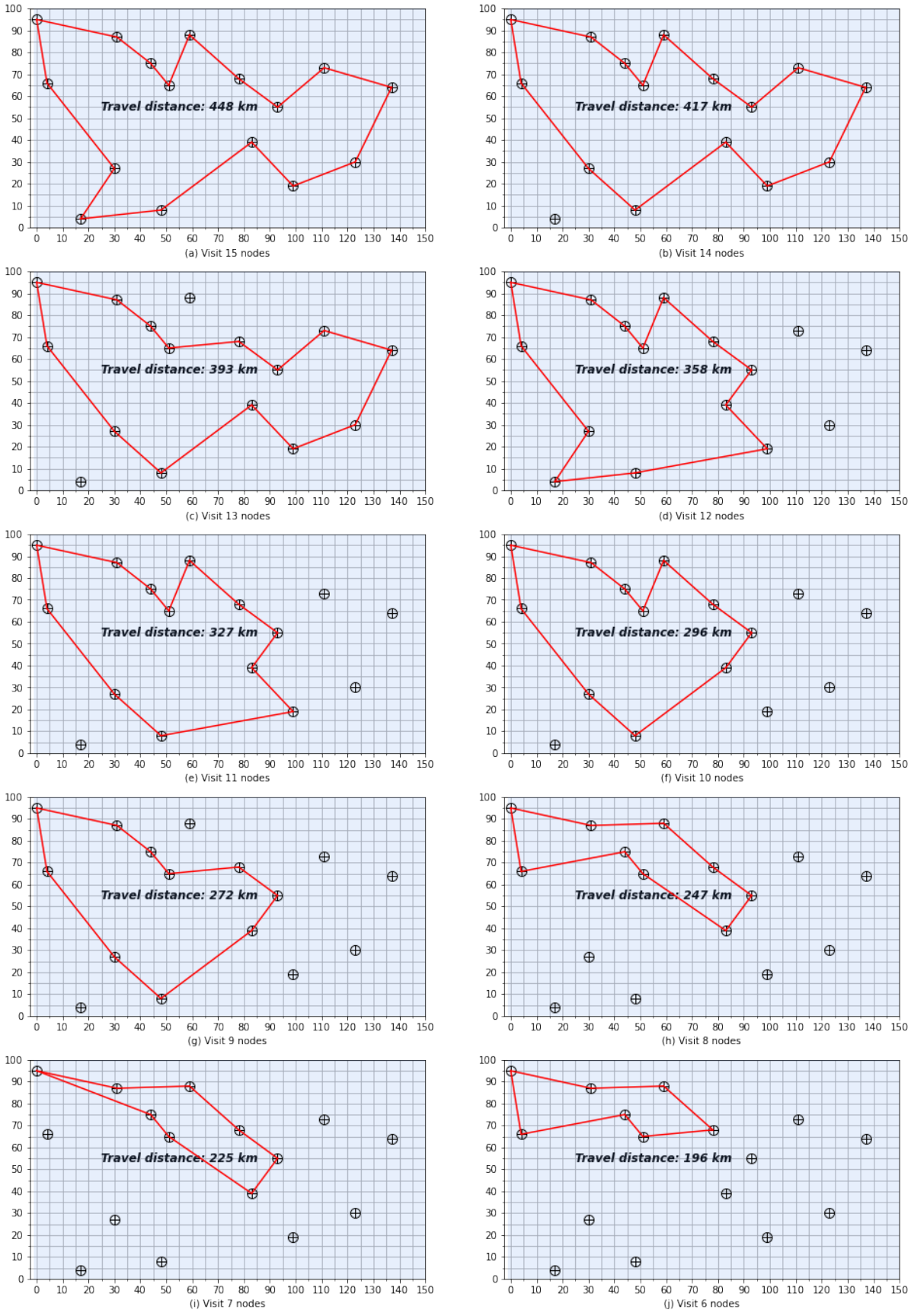

Figure 13 Patrol routes with different numbers of visiting nodes in Scenario 2

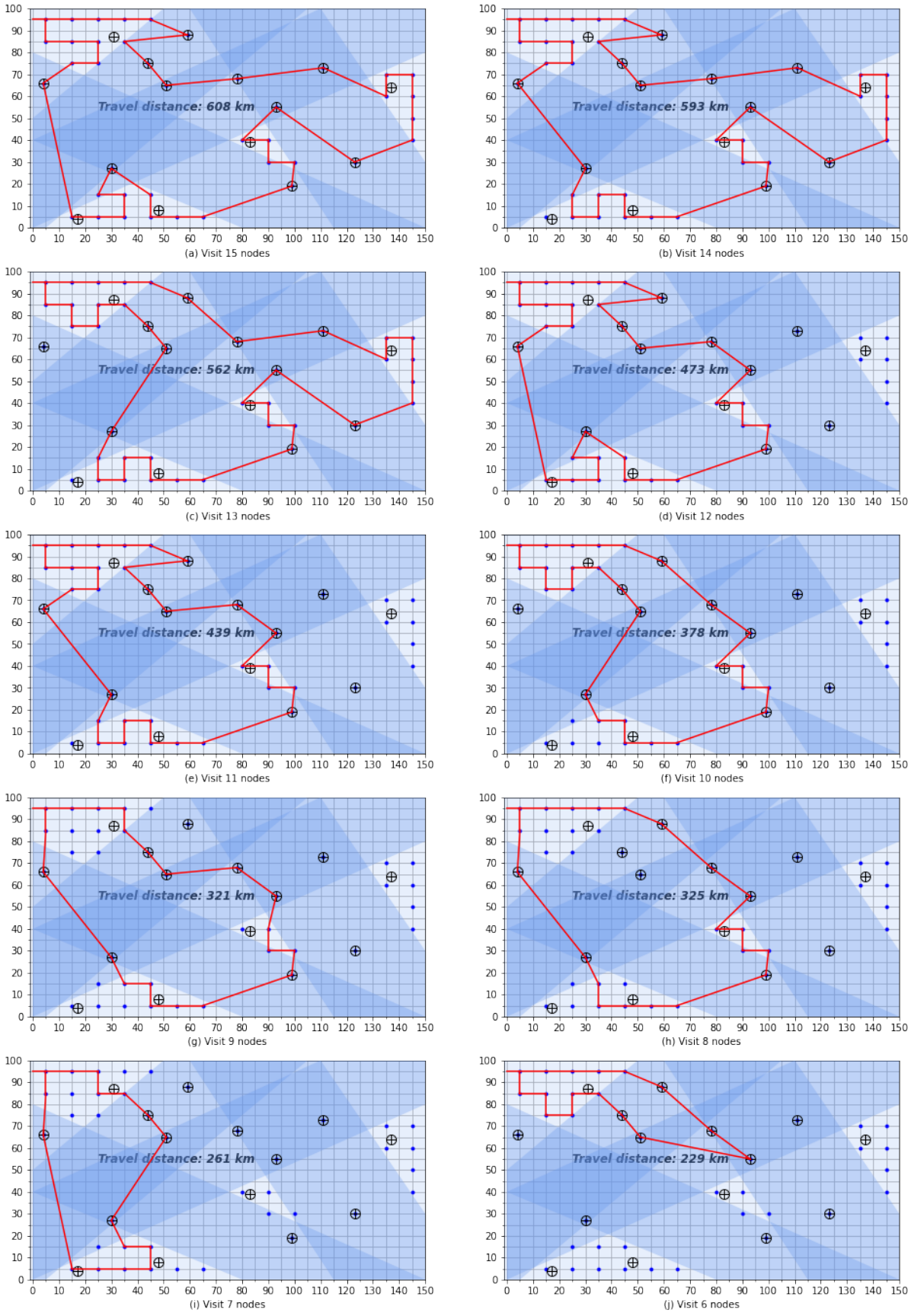

Figure 14 Patrol routes with different numbers of visiting nodes in Scenario 3

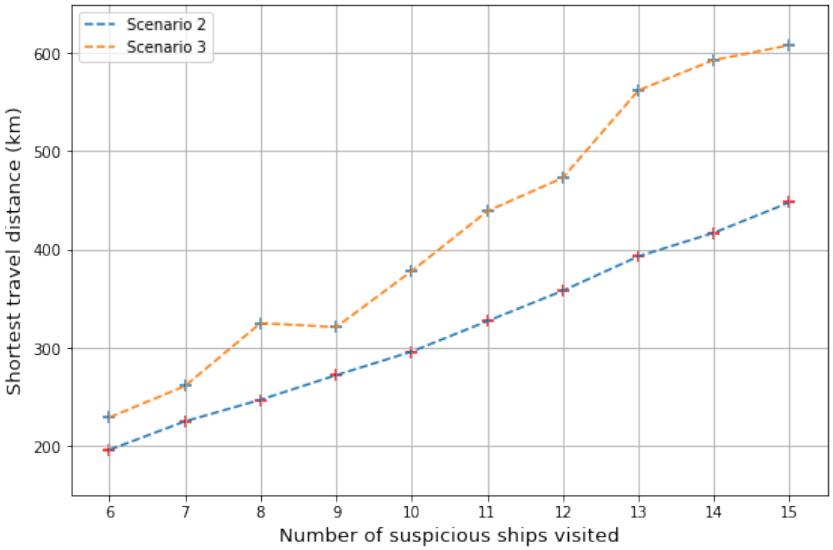

Figure 15 Shortest travel distance to visit a certain number of suspicious ships

Table 3 Number of nodes that can be visited under different travel distance constraints

Travel distance (km)	Instance 1			Instance 2			Instance 3		
	Scenario 2	Scenario 3	Gap	Scenario 2	Scenario 3	Gap	Scenario 2	Scenario 3	Gap
200	4	3	1	5	3	2	5	4	1
300	9	5	4	10	6	4	9	7	2
400	13	8	4	13	9	3	13	10	3
500	**15**	10	5	**15**	9	6	**15**	11	4

3.2.1. Sensitivity analysis

Considering that even in maritime crime hotspots, the available data suggest that only 0.1 fishery-related and piracy-related offenses are reported on average per day, we believe the actual extent of maritime crimes is largely unknown. Therefore, it is necessary to further explore Scenario 3 with different numbers and distribution patterns of suspicious ships. We set the number of suspicious ships (i.e., $|V|$) in the inspection area as 8, 10, 12, and 15, respectively. These numbers were chosen following consultation with researchers focusing on maritime and water security at several institutes for security studies and estimates that they provided. Moreover, to better reflect the real-world situation (i.e., crime decreases with increased distance from shorelines), we also study the influence of both even and uneven distribution patterns. Table 4 provides two specific distribution patterns, in which D1 and D2 represent the uneven and even distribution patterns, respectively.

Table 4 Probability distribution of suspicious ships at seas

Distance from shorelines (km)		(0, 50]	(50, 100]	(100, 150]
D1	Probability function	0.6	0.3	0.1
	Cumulative probability function	0.6	0.9	1
D2	Probability function	0.33	0.33	0.33
	Cumulative probability function	0.33	0.66	1

We then perform 80 experiments to further investigate Scenario 3. The parameters settings are as follows. Given $|V|$, we generate 10 random cases and let α denote the index of a case. The suspicious ships are randomly distributed in the marine conservation areas. The location of suspicious ships is generated based on the distribution functions, i.e., D1 or D2, defined in Table 4. The other parameters are the same as the previous setting. For notational simplicity, we denote a case by $|V|(\alpha)-\mathrm{D}\beta$, where $|V|$ denotes the number of suspicious ships, α denotes the index for the case in a group of cases that share the same $|V|$, and $\mathrm{D}\beta$ denotes the distribution pattern defined in Table 4.

The results for these cases are reported in Table 5. In this table, the performance of the model is reflected by the number of inspected ships, which is reported in the column labeled "No. of inspected ships". The relative performance is measured by the percentage of inspected ships which is defined as $100\% \times (|V'|/|V|)$ and reported in the column labeled "Inspection percentage." In this formula, V' denotes the set of inspected ships and $|V'|$ denotes the set of all suspicious ships. The travel distance of each patrol is also derived and reported in the column labeled "Patrol distance."

As expected, the patrol efficiency is higher when the suspicious ships are unevenly distributed. This phenomenon becomes more obvious as the number of suspicious ships, i.e., $|V|$, increases. For example, in the group 15-D1, an average of 11.9 ships (i.e., 79% of the ships) are inspected. By comparison, only an average of 9.6 ships (i.e., 64%) are inspected in the group 15-D2. Considering the uneven distribution pattern (i.e., D1) yields a higher distribution density in offshore waters and our proposed model can adaptively select the inspection spots, it is not surprising the uneven distribution pattern achieves better inspection efficiency. However, this phenomenon is not obvious, when $|V|$ is small. In this study, when $|V| \leq 10$,

the difference between D1 and D2 is not obvious, mainly because the density of suspicious ships in both distributions is too sparse.

We also check the travel distance of each patrol route. The travel distance of all patrol routes is equal to or close to the travel distance limitation, which further demonstrates that the proposed model can maximize the objective of improving the inspection performance by fully utilizing the given travel distance range.

Table 5 Results of instances in Scenario 3.

Instance	No. of inspected ships	Inspection percentage	Patrol distance	Instance	No. of inspected ships	Inspection percentage	Patrol distance
15(1)-D1	11	73%	496	15(1)-D2	10	67%	499
15(2)-D1	12	80%	499	15(2)-D2	8	53%	500
15(3)-D1	11	73%	497	15(3)-D2	11	73%	499
15(4)-D1	11	73%	497	15(4)-D2	10	67%	499
15(5)-D1	14	93%	499	15(5)-D2	10	67%	499
15(6)-D1	10	67%	499	15(6)-D2	9	60%	499
15(7)-D1	14	93%	499	15(7)-D2	10	67%	498
15(8)-D1	13	87%	496	15(8)-D2	11	73%	497
15(9)-D1	11	73%	499	15(9)-D2	8	53%	499
15(10)-D1	12	80%	499	15(10)-D2	9	60%	499
15-D1-Min	10	67%	496	15-D2-Min	8	53%	497
15-D1-Max	14	93%	499	15-D2-Max	11	73%	500
15-D1-Ave	11.9	79%	498	15-D2-Ave	9.58	64%	498.8
12(1)-D1	9	75%	495	12(1)-D2	4	33%	500
12(2)-D1	8	67%	497	12(2)-D2	10	83%	499
12(3)-D1	7	58%	500	12(3)-D2	8	67%	499
12(4)-D1	6	50%	500	12(4)-D2	8	67%	500
12(5)-D1	10	83%	498	12(5)-D2	7	58%	498
12(6)-D1	9	75%	500	12(6)-D2	7	58%	496
12(7)-D1	8	67%	500	12(7)-D2	5	42%	498
12(8)-D1	10	83%	497	12(8)-D2	7	58%	499
12(9)-D1	9	75%	498	12(9)-D2	6	50%	498
12(10)-D1	7	58%	499	12(10)-D2	5	42%	497
12-D1-Min	6	50%	495	12-D2-Min	4	33%	496
12-D1-Max	10	83%	500	12-D2-Max	10	83%	500
12-D1-Ave	8.3	69%	498.4	12-D2-Ave	6.7	56%	498.4
10(1)-D1	7	70%	500	10(1)-D2	6	60%	500

10(2)-D1	8	80%	499	10(2)-D2	7	70%	497
10(3)-D1	8	80%	499	10(3)-D2	9	90%	498
10(4)-D1	5	50%	495	10(4)-D2	6	60%	499
10(5)-D1	6	60%	496	10(5)-D2	7	70%	497
10(6)-D1	9	90%	500	10(6)-D2	7	70%	499
10(7)-D1	8	80%	499	10(7)-D2	8	80%	500
10(8)-D1	7	70%	499	10(8)-D2	5	50%	495
10(9)-D1	9	90%	500	10(9)-D2	6	60%	499
10(10)-D1	6	60%	498	10(10)-D2	7	70%	496
10-D1-Min	5	50%	495	10-D2-Min	5	50%	495
10-D1-Max	9	90%	500	10-D2-Max	9	90%	500
10-D1-Ave	7.3	73%	498.5	10-D2-Ave	6.8	68%	498
8(1)-D1	5	63%	498	8(1)-D2	6	75%	499
8(2)-D1	7	88%	500	8(2)-D2	7	88%	499
8(3)-D1	7	88%	495	8(3)-D2	7	88%	497
8(4)-D1	5	63%	497	8(4)-D2	6	75%	498
8(5)-D1	4	50%	499	8(5)-D2	5	63%	499
8(6)-D1	6	75%	500	8(6)-D2	7	88%	500
8(7)-D1	7	88%	499	8(7)-D2	6	75%	499
8(8)-D1	7	88%	497	8(8)-D2	5	63%	498
8(9)-D1	5	63%	499	8(9)-D2	5	63%	495
8(10)-D1	7	88%	500	8(10)-D2	7	88%	499
8-D1-Min	4	50%	495	8-D2-Min	5	63%	495
8-D1-Max	7	88%	500	8-D2-Max	7	88%	500
8-D1-Ave	6	75%	498.4	8-D2-Ave	6.1	76%	498.3

4. Conclusions

Patrol is of great importance to fight maritime crimes, improve maritime security, and protect the maritime ecosystem and industry. We study a patrol routing problem to maximize the efficiency of maritime patrolling and prevent maritime crimes, i.e., detect and inspect as many suspicious ships as possible, by appropriately planning a patrol route. We are the first to study the benefit of using a novel suspicious ship sensing approach, i.e., the joint application of AP and AIS, in maritime patrolling. To this end, we consider three scenarios for this problem based on the availability of AIS-AP support. We build tailored model for each scenario. Numerical experiments are conducted, and the results demonstrate that the proposed patrol routes using AIS and AP (in Scenarios 2 and 3) greatly enhance the efficiency of maritime patrolling.

Our study is of significant value to maritime affairs authorities, especially in areas with a high risk of maritime crimes. Our approach can enable maritime authorities to create appropriate route plans for their patrol boats, including choosing the regions or locations to visit, creating visit sequences, defining the scope of the visits, and determining the required travel distances. Maritime authorities can also select the optimal patrol routes based on the different travel distances and work hour requirements. In other words, they can plan the best patrol routes for different scenarios and performance requirements. The proposed patrol route planning method can increase the efficiency and reduce the consumption of resources (e.g., the workload of inspectors and the number of patrol boats) on maritime patrol missions. For further study, multiple-ship patrols should be considered for the maritime patrol routing problem, which has been demonstrated to be NP-Hard. Special attention should be paid to the complexity of the solution algorithm. An efficient algorithm should also be developed to resolve the maritime patrol routing problem for real-sized cases.

References

Bahrami, S., Nourinejad, M., Amirjamshidi, G., Roorda, M.J., 2020. The plugin hybrid electric vehicle routing problem: A power-management strategy model. *Transportation Research Part C: Emerging Technologies* 111, 318-333.

Basso, R., Kulcsár, B., Sanchez-Diaz, I., Qu, X., 2022. Dynamic stochastic electric vehicle routing with safe reinforcement learning. *Transportation Research Part E: Logistics and Transportation Review* 157, 102496.

Belhabib, D., Sumaila, U.R., Le Billon, P., 2019. The fisheries of Africa: Exploitation, policy, and maritime security trends. *Marine Policy* 101, 80-92.

Bueger, C., 2015. What is maritime security? *Marine Policy* 53, 159-164.

Bueger, C., Edmunds, T.J.I.A., 2017. Beyond seablindness: a new agenda for maritime security studies. *International Affairs* 93(6), 1293-1311.

Çapar, İ., Keskin, B.B., Rubin, P.A., 2015. An improved formulation for the maximum coverage patrol routing problem. *Computers & Operations Research* 59, 1-10.

611 Chen, H., Cheng, T., Wise, S., 2017. Developing an online cooperative police patrol routing
612 strategy. *Computers, Environment and Urban Systems* 62, 19-29.
613 Daganzo, C.F., 1984. The length of tours in zones of different shapes. *Transportation Research*
614 *Part B: Methodological* 18(2), 135-145.
615 De Santo, E.M., 2020. Militarized marine protected areas in overseas territories: Conserving
616 biodiversity, geopolitical positioning, and securing resources in the 21st century. *Ocean*
617 *& Coastal Management* 184, 105006.
618 Dewil, R., Vansteenwegen, P., Cattrysse, D., Van Oudheusden, D., 2015. A minimum cost
619 network flow model for the maximum covering and patrol routing problem. *European*
620 *Journal of Operational Research* 247(1), 27-36.
621 Duan, G., Fan, T., Chen, L., Ma, J., 2021. Floating marine debris mitigation by vessel routing
622 modeling and optimization considering carbon emission and travel time.
623 *Transportation Research Part C: Emerging Technologies* 133, 103449.
624 Frederiksen, P., Morf, A., von Thenen, M., Armoskaite, A., Luhtala, H., Schiele, K.S., Strake,
625 S., Hansen, H.S., 2021. Proposing an ecosystem services-based framework to assess
626 sustainability impacts of maritime spatial plans (MSP-SA). *Ocean & Coastal*
627 *Management* 208, 105577.
628 Gallego, A.-J., Pertusa, A., Gil, P., 2018. Automatic ship classification from optical aerial
629 images with convolutional neural networks. *Remote Sensing* 10(4).
630 Germond, B., 2015. The geopolitical dimension of maritime security. *Marine Policy* 54, 137-
631 142.
632 Gmira, M., Gendreau, M., Lodi, A., Potvin, J.-Y., 2021. Managing in real-time a vehicle
633 routing plan with time-dependent travel times on a road network. *Transportation*
634 *Research Part C: Emerging Technologies* 132, 103379.
635 Gonzalez-R, P.L., Canca, D., Andrade-Pineda, J.L., Calle, M., Leon-Blanco, J.M., 2020.
636 Truck-drone team logistics: A heuristic approach to multi-drop route planning.
637 *Transportation Research Part C: Emerging Technologies* 114, 657-680.

638 Guilfoyle, D., 2019. The rule of law and maritime security: understanding lawfare in the South
639 China Sea. *International Affairs* 95(5), 999-1017.
640 ICC, 2022. Gulf of Guinea records highest ever number of crew kidnapped in 2020, according
641 to IMB's annual piracy report. https://www.icc-ccs.org/index.php/1301-gulf-of-
642 guinea-records-highest-ever-number-of-crew-kidnapped-in-2020-according-to-imb-s-
643 annual-piracy-report. Accessed 5 July 2022.
644 ICPO, 2019. Marine pollution: thousands of serious offences exposed in global operation.
645 https://www.interpol.int/News-and-Events/News/2019/Marine-pollution-thousands-
646 of-serious-offences-exposed-in-global-operation. Accessed 15 March 2022.
647 ICPO, 2020. Project Compass. https://www.interpol.int/Crimes/Maritime-crime/Project-
648 Compass. Accessed 15 March 2022.
649 ICPO, 2021a. Project MAST, Southeast Asia. https://www.interpol.int/Crimes/Maritime-
650 crime/Project-MAST-Southeast-Asia. Accessed 17 March 2022.
651 ICPO, 2021b. Red Sea Initiative. https://www.interpol.int/Crimes/Maritime-crime/Red-Sea-
652 Initiative. Accessed 16 March 2022.
653 Keskin, B.B., Li, S., Steil, D., Spiller, S., 2012. Analysis of an integrated maximum covering
654 and patrol routing problem. *Transportation Research Part E: Logistics and*
655 *Transportation Review* 48(1), 215-232.
656 Laporte, G., Martello, S., 1990. The selective travelling salesman problem. *Discrete Applied*
657 *Mathematics* 26(2), 193-207.
658 Li, M., Xie, C., Li, X., Karoonsoontawong, A., Ge, Y.-E., 2022. Robust liner ship routing and
659 scheduling schemes under uncertain weather and ocean conditions. *Transportation*
660 *Research Part C: Emerging Technologies* 137, 103593.
661 Li, S., Keskin, B.B., 2014. Bi-criteria dynamic location-routing problem for patrol coverage.
662 *Journal of the Operational Research Society* 65(11), 1711-1725.
663 Lin, B., Ghaddar, B., Nathwani, J., 2021. Electric vehicle routing with charging/discharging
664 under time-variant electricity prices. *Transportation Research Part C: Emerging*
665 *Technologies* 130, 103285.

666 Liu, X., Qu, X., Ma, X., 2021. Improving flex-route transit services with modular autonomous
667 vehicles. *Transportation Research Part E: Logistics and Transportation Review* 149,
668 102331.
669 Menegon, S., Depellegrin, D., Farella, G., Sarretta, A., Venier, C., Barbanti, A., 2018.
670 Addressing cumulative effects, maritime conflicts and ecosystem services threats
671 through MSP-oriented geospatial webtools. *Ocean & Coastal Management* 163, 417-
672 436.
673 Miller, C.E., Tucker, A.W., Zemlin, R.A., 1960. Integer programming formulation of traveling
674 salesman problems. *Journal of the ACM* 7(4), 326-329.
675 MSC, 2022. Oceans at risk. https://www.msc.org/en-au/what-we-are-doing/oceans-at-risk.
676 Accessed 5 July 2022.
677 Nordling, L., 2017. South Africa tackles crime at sea with ship-spotting satellites.
678 https://doi.org/10.1038/nature.2017.22977. Accessed 15 August 2021.
679 Okafor-Yarwood, I., 2020. The Cyclical Nature of Maritime Security Threats: Illegal,
680 Unreported, and Unregulated Fishing as a Threat to Human and National Security in
681 the Gulf of Guinea. *African Security* 13(2), 116-146.
682 Poon, M., Gu, R., Yuan, Y., 2022. A vehicle routing problem with option for outsourcing and
683 time-dependent travel time. *IEEE Access* 10, 49757-49770.
684 Portugal, D., Rocha, R.P., 2013. Distributed multi-robot patrol: A scalable and fault-tolerant
685 framework. *Robotics and Autonomous Systems* 61(12), 1572-1587.
686 Qi, M., Hao, X., Yuan, M., 2022. An optimal layout pattern-based solution approach to the
687 extended machine layout problem with multirow multicolumn structure. *IEEE*
688 *Transactions on Automation Science and Engineering*, 1-21.
689 Ryan, B.J., 2019. The disciplined sea: a history of maritime security and zonation. *International*
690 *Affairs* 95(5), 1055-1073.
691 Stable Seas, 2019. Stable Seas: Sulu and Celebes Seas. https://www.stableseas.org/post/stable-
692 seas-sulu-and-celebes-seas. Accessed 8 April 2022.

693 Steil, D.A., Pate, J.R., Kraft, N.A., Smith, R.K., Dixon, B., Ding, L., Parrish, A., 2011. Patrol
694 Routing Expression, Execution, Evaluation, and Engagement. *IEEE Transactions on*
695 *Intelligent Transportation Systems* 12(1), 58-72.
696 UNFAO, 2020. State of World Fisheries and Aquaculture (SOFIA) report.
697 https://www.fao.org/publications/sofia/2020/en/. Accessed 5 July 2022.
698 UNODC, 2011. Transnational organized crime in the fishing industry.
699 https://www.unodc.org/documents/human-trafficking/Issue_Paper_-
700 _TOC_in_the_Fishing_Industry.pdf. Accessed 1 April 2022.
701 UNODC, 2021. Maritime Crime and Piracy. https://www.unodc.org/romena/en/maritime-
702 crime-and-piracy.html. Accessed 25 March 2022.
703 Vidal, T., Maculan, N., Ochi, L.S., Penna, P.H.V., 2016. Large Neighborhoods with Implicit
704 Customer Selection for Vehicle Routing Problems with Profits. *Transportation Science*
705 50(2), 720-734.
706 Voyer, M., Quirk, G., McIlgorm, A., Azmi, K., 2018a. Shades of blue: what do competing
707 interpretations of the Blue Economy mean for oceans governance? *Journal of*
708 *Environmental Policy & Planning* 20(5), 595-616.
709 Voyer, M., Schofield, C., Azmi, K., Warner, R., McIlgorm, A., Quirk, G., 2018b. Maritime
710 security and the Blue Economy: intersections and interdependencies in the Indian
711 Ocean. *Journal of the Indian Ocean Region* 14(1), 28-48.
712 Wang, Y., Peng, S., Zhou, X., Mahmoudi, M., Zhen, L., 2020. Green logistics location-routing
713 problem with eco-packages. *Transportation Research Part E: Logistics and*
714 *Transportation Review* 143, 102118.
715 Willemse, E.J., Joubert, J.W., 2012. Applying min–max k postmen problems to the routing of
716 security guards. *Journal of the Operational Research Society* 63(2), 245-260.
717 WWF, 2015. Living Blue Planet Report 2015.
718 http://assets.wwf.org.uk/custom/stories/living_blue_planet/. Accessed 5 July 2022.

719 Zeng, F., Chen, Z., Clarke, J.-P., Goldsman, D., 2022. Nested vehicle routing problem:
720 Optimizing drone-truck surveillance operations. *Transportation Research Part C:*
721 *Emerging Technologies* 139, 103645.
722 Zhang, W., Wang, K., Wang, S., Laporte, G., 2020. Clustered coverage orienteering problem
723 of unmanned surface vehicles for water sampling. *Naval Research Logistics* 67(5), 353-
724 367.
725 Zhen, L., Hu, Z., Yan, R., Zhuge, D., Wang, S., 2020. Route and speed optimization for liner
726 ships under emission control policies. *Transportation Research Part C: Emerging*
727 *Technologies* 110, 330-345.
728